Atmos. Chem. Phys. Discuss., doi:10.5194/acp-2016-50, 2016
Manuscript under review for journal Atmos. Chem. Phys.
Published: 1 March 2016


# Chamber simulation on the formation of secondary organic aerosols (SOA) from diesel vehicle exhaust in China

Wei Deng[1,2], Qihou Hu[1], Tengyu Liu[1,2], Xinming Wang[1,*], Yanli Zhang[1], Xiang Ding[1], Yele Sun[3], Xinhui Bi[1], Jianzhen Yu[4], Weiqiang Yang[1,2], Xinyu Huang[1,2], Zhou Zhang[1,2], Zhonghui Huang[1,2], Quanfu He[1,2], A. Mellouki[5], Christian George[6]

[1]State Key Laboratory of Organic Geochemistry and Guangdong Key Laboratory of Environmental Protection and Resources Utilization, Guangzhou Institute of Geochemistry, Chinese Academy of Sciences, Guangzhou 510640, China

[2]University of Chinese Academy of Sciences, Beijing 100049, China

[3]Institute of Atmospheric Physics, Chinese Academy of Sciences, Beijing 100029, China

[4]Division of Environment, Hong Kong University of Science & Technology, Clear Water Bay, Kowloon, Hong Kong, China

[5]Institut de Combustion, Aérothermique, Réactivité et Environnement (ICARE), CNRS, 45071 Orléans cedex 02, France

[6]Institut de Recherches sur la Catalyse et l'Environnement de Lyon (IRCELYON), CNRS, UMR5256, Villeurbanne F-69626, France

*Corresponding author:

Dr. Xinming Wang

State Key Laboratory of Organic Geochemistry

Guangzhou Institute of Geochemistry, Chinese Academy of Sciences

Tel: +86-20-85290180; Fax: +86-20-85290706

Email: wangxm@gig.ac.cn

Atmos. Chem. Phys. Discuss., doi:10.5194/acp-2016-50, 2016
Manuscript under review for journal Atmos. Chem. Phys.
Published: 1 March 2016


**Abstract**

In China primary particulate matter emission from on-road vehicles is predominantly coming from diesels, yet secondary organic aerosols (SOA) formed from diesel emission may be also of greater significance due to more intermediate volatile organic compounds (IVOC) in the exhaust. Here we introduced exhaust from in-use diesel vehicles under warm idling condition directly into an indoor smog chamber with a 30m$^3$ Teflon reactor, and investigated the SOA formation as well as chemical aging of organic aerosols during photo-oxidation. The emission factors of primary organic aerosol (POA) and black carbon (BC) for the three typical Chinese diesel vehicles ranged 0.18-0.91 and 0.15-0.51 g kg-fuel$^{-1}$, respectively; and the SOA production factors ranged 0.50-1.8 g kg-fuel$^{-1}$ with an average SOA/POA ratio of 1.6. Aromatic hydrocarbons could only explain less than 3% of SOA formed during aging, and IVOC and oxygenated VOC might contribute substantially to SOA formation. High resolution time-of-flight aerosol mass spectrometer (HR-ToF-AMS) resolved that POA dominated by CH classes (alkanes, cycloalkanes and alkenes) with high abundances of the $C_nH_{2n+1}$ and $C_nH_{2n-1}$ fragments, and after photo-oxidation the fraction of CH classes and the H/C ratios decreased, while the fraction of CHO, as well as the ratios of O/C and of organic matter to organic carbon (OM/OC), all increased. The plot of $f_{44}$ (ratio of *m/z* 44 to the total signal in a mass spectrum) versus $f_{43}$ indicated that diesel SOA were semi-volatile oxygenated organic aerosols (SV-OOA). The slopes of O:C versus H:C element ratios in the Van Krevelen diagram ranged from -0.47 to -0.68, suggesting a combination of carboxylic acid and

Atmos. Chem. Phys. Discuss., doi:10.5194/acp-2016-50, 2016
Manuscript under review for journal Atmos. Chem. Phys.
Published: 1 March 2016


alcohols/peroxides formed during the aging of diesel exhaust.

Atmos. Chem. Phys. Discuss., doi:10.5194/acp-2016-50, 2016
Manuscript under review for journal Atmos. Chem. Phys.
Published: 1 March 2016


## 1 Introduction

Air pollution by particulate matter not only adversely affects human health by causing respiratory and cardiopulmonary diseases (Pope et al., 2009; Brook et al., 2010; Liu et al., 2015b; Lelieveld et al., 2015), but also impacts regional and global climate (Ramanathan et al., 2001; Parrish and Zhu, 2009; Wang et al., 2014b). Health risks are of particular concern when heavy fine particle (particulate matter with dynamic diameter less than 2.5 μm, $PM_{2.5}$) pollution occurs in densely populated megacities, such as China's capital city Beijing, which is hard-hit by frequent heavy haze episodes with a large body of people exposed to severe $PM_{2.5}$ pollution (Guo et al., 2014; Huang et al., 2014). In urban agglomerations, vehicle exhaust contributes substantially to $PM_{2.5}$, with mass fractions ranging from ~22% in southeastern US (Chen et al., 2012), ~37% in Guangzhou in the Pearl River Delta during wet season (Cui et al., 2015), to as high as 49% in Mexico City (Stone et al., 2008). In particular, People usually expose to much higher air pollutants in urban roadside microenvironments due to traffic-related emission (Zhao et al., 2004; Xu et al., 2008). Nevertheless, the contribution of vehicle exhaust to $PM_{2.5}$ is often a debatable issue. In Beijing, for example, previous studies revealed that contributions of vehicle exhaust to $PM_{2.5}$ might range from 4% to 16.3% (Zheng et al., 2005; Song et al., 2006a, b, 2007b; Zhang et al., 2013; Wu et al., 2014), whilst very recently Beijing Municipal Environmental Protection Bureau announced that vehicle exhaust alone accounted for 31% of $PM_{2.5}$ mass (http://www.bjepb.gov.cn/bjepb/413526/331443/331937/333896/396191/index.html). One crucial reason for the discrepancies is the

Atmos. Chem. Phys. Discuss., doi:10.5194/acp-2016-50, 2016
Manuscript under review for journal Atmos. Chem. Phys.
Published: 1 March 2016


lack of understanding about secondary aerosols formed from vehicle exhaust.

Direct motor vehicle emission of PM is predominantly from diesel vehicles (Reff et al., 2009; Zhang et al., 2009). In China diesel vehicles contributed more than 99% of primary vehicle emission of PM although they only account for 15.2% of China's on-road vehicles (MEPC, 2014). Recent studies in Beijing revealed that diesel vehicles contribute 80%–90% of PM emissions from on-road sources (Huo et al., 2011; Wu et al., 2010; Wang et al., 2010). Hence, restriction of diesel vehicles into the core urban areas has become a control measure widely adopted by municipal governments to improve air quality. Besides primary particle emission, vehicle exhaust also contributes substantially to gaseous pollutants, such as volatile organic compounds (VOCs) and nitrogen oxides ($NO_x$), which can form secondary organic and inorganic aerosols via photo-oxidation (Weitkamp et al., 2007; Robinson et al., 2007; Nordin et al., 2013; Liu et al., 2015a). Nordin et al. (2013) reported that secondary organic aerosols (SOA) formed from gasoline exhaust can reach as high as 500 times that of primary organic aerosols (POA). Although primary PM emission factors of diesel vehicles are typically orders of magnitude higher than gasoline vehicles, recent studies demonstrated that for diesel vehicles the SOA/POA ratios could reach about 3 based on chamber simulations (Chirico et al., 2010; Gordon et al., 2014b). Consequently, contribution of vehicle exhaust to ambient fine particles would become more complicated if considering secondary aerosol formation.

In China, a large portion of gasoline vehicles are produced in Sino-Foreign joint ventures and due to transfer of gasoline engine technology from abroad, chamber

Atmos. Chem. Phys. Discuss., doi:10.5194/acp-2016-50, 2016
Manuscript under review for journal Atmos. Chem. Phys.
Published: 1 March 2016


simulation study showed that the SOA/POA ratios for China's gasoline vehicle exhaust are quite similar with those reported in the Europe or in the US (Liu et al., 2015a). However, engines equipped on China's diesel vehicles are mainly designed and produced domestically with their technology lagging behind the developed nations. According to previous studies (Yanowitz, 2000; Cheung et al., 2009; Liu et al., 2009), the emission factors of both hydrocarbon and particulate matter for diesel vehicles in China were much higher than those in the developed nations. Therefore, the SOA formation from China's diesel exhaust may be different with those in Europe and the US as well. Furthermore, most diesel vehicles in China are not equipped with emission control aftertreatment devices, which can significantly reduce both POA emission and SOA formation (Chirico et al., 2010; Gordon et al., 2014b). As previous study indicates that even for diesel vehicles SOA might dominate over POA, formation of SOA from diesel vehicles in China would be an issue of wide concern.

In this study, we chose three typical types of diesel vehicles made in China, introduced the exhaust from the diesel vehicles under warm idling condition into an indoor smog chamber with a 30 $m^3$ reactor, and investigated the SOA formation under photo-oxidation. The main purpose of this study is to obtain a more comprehensive evaluation of diesel vehicle's contribution to carbonaceous aerosols by studying SOA formation from the primarily emitted exhaust.

## 2 Materials and methods

### 2.1 Vehicles and fuel

Table 1 lists the three diesel vehicles used for our chamber experiments. They

Atmos. Chem. Phys. Discuss., doi:10.5194/acp-2016-50, 2016
Manuscript under review for journal Atmos. Chem. Phys.
Published: 1 March 2016


represent three different types of diesel vehicles manufactured by three major diesel vehicle makers in China. Foton is a medium-duty passenger vehicle made by the Baic Motor Corporation LTD., Changan is a medium-duty truck made by the China Changan Automobile Group, and JAC is a heavy-duty truck made by the JAC Motors. In 2011, the diesel vehicle productions of the three companies were 490,280, 299,506 and 230,452, respectively (China Automotive Industry Yearbook, 2012), and their diesel vehicle sales were all among the top 10 in China. All the vehicles in this study had no exhaust aftertreatment devises and they were fueled with Grade 0# diesel, which complies with the Euro III diesel fuel standard.

**2.2 Experimental setup**

The experiments were carried out in the indoor smog chamber at Guangzhou Institute of Geochemistry, Chinese Academy of Sciences (GIG-CAS) with a ~30 $m^3$ Teflon reactor suspended in a temperature-controlled room. Details of setup and facilities about the chamber were described elsewhere (Wang et al., 2014a). Briefly, 135 black lamps (1.2 m long, 60 W Philips/ 10R BL, Royal Dutch Philips Electronics Ltd., the Netherlands) are used as light source, providing a $NO_2$ photolysis rate of 0-0.49 $min^{-1}$. Temperature can be set in a range from -10 to 40°C with an accuracy of ±1°C, and is measured by eight sensors inside the enclosure and the other one inside the Teflon reactor. In this study, temperature and relative humidity (RH) for all experiment were set to 25°C and less than 5%, respectively. Prior to each experiment, the Teflon chamber was flushed with dry purified air for at least 48 hours, which represents at least 5 whole exchanges of the reactor volume. Before each experiment, the chamber

Atmos. Chem. Phys. Discuss., doi:10.5194/acp-2016-50, 2016
Manuscript under review for journal Atmos. Chem. Phys.
Published: 1 March 2016


was checked for hydrocarbons, ozone, $NO_x$, and particles inside the reactor to make sure it was clean.

Before introducing exhaust into the chamber reactor, all vehicles in the experiments were at "warm idling" mode, which means the vehicles were started and run on-road for about 30min before staying at idling condition. Depending on the organic aerosol concentration and particle numbers reached inside the reactor as sensed by the affiliated instruments, the exhaust injection time ranged from 5 to 20 min.

After introducing exhausts, nitrous acid (HONO) was bubbled into the chamber as a source of hydroxyl radical (OH). Propene was added to adjust the VOC/$NO_x$ ratios to approximately 3:1 ppbC:ppb. Propene has often been added to adjust VOC/$NO_x$ ratio in diesel exhaust chamber experiments (Chirico et al., 2010; Presto et al., 2014; Gordon et al., 2014b) and is not considered to be a relevant SOA precursor (Odum et al., 1996; Coker et al., 2001). 60 ppbv of deuterated butanol (butanol-d9) was also injected into the chamber as an OH tracer by using $k_{\text{butanol-d9}} = 3.4\times10^{-12}$ $cm^3$ $molecule^{-1}s^{-1}$ (Barmet et al., 2012; Gordon et al., 2014a). After characterizing the primary emissions in a dark condition for an hour, the exhaust was photo-oxidized for 5 h by being exposed to black lights.

### 2.3 Instrumentation

An array of instruments was used to monitoring trace gases and particles inside the chamber. Ozone ($O_3$) was measured with an ozone analyzer (EC9810, Ecotech, Australia) and $NO_x$ were measured with a trace nitrogen oxides analyzer (EC9841, Ecotech, Australia). $SO_2$ was measured with a dedicated analyzer (Model 43i, Thermo

Atmos. Chem. Phys. Discuss., doi:10.5194/acp-2016-50, 2016
Manuscript under review for journal Atmos. Chem. Phys.
Published: 1 March 2016


Scientific, USA). VOCs were measured online with a commercial proton-transfer-reaction time-of-flight mass spectrometer (PTR-TOF-MS, Model 2000, Ionicon Analytik GmbH, Austria) (Lindinger et al., 1998; Jordan et al., 2009). Offline VOC samples were also collected using 2L stainless steel canisters each 30 min during the photo-oxidation, and measured by a Model 7100 Preconcentrator (Entech Instruments Inc., California, USA) coupled with an Agilent 5973N gas chromatography-mass selective detector/flame ionization detector (GC-MSD/FID, Agilent Technologies, USA). CO in the canister samples was analyzed using a gas chromatography (6980GC, Agilent, USA) with a flame ionization detector and a packed column (5A molecular sieve 60/80 mesh, 3 m×1/8 inch). Detailed procedures for the offline analysis of VOCs and CO were described elsewhere (Zhang et al., 2012). Before and after introducing exhaust, air samples were collected into 3L cleaned Teflon bags to determine $CO_2$ concentrations with an HP 4890D gas chromatography (Yi et al., 2007).

A scanning mobility particle sizer (SMPS, Model 3080 classifier, model 3775 CPC; TSI Inc., Minnesota, USA) was used to measure particle number and volume concentrations and size distributions. The particle mass concentration was estimated assuming spherical particles and a density of 1.0 g $cm^{-3}$ (Weitkamp et al., 2007). BC concentrations were measured with a seven-channel Aethalometer (Model AE-31, Magee Scientific, Berkeley, California). The Aethalometer data were corrected for particle loading effects using the method of Kirchstetter and Novakov (2007). A high-resolution time-of-flight aerosol mass spectrometer (HR-ToF-MS, Aerodyne

Atmos. Chem. Phys. Discuss., doi:10.5194/acp-2016-50, 2016
Manuscript under review for journal Atmos. Chem. Phys.
Published: 1 March 2016


Research Inc., USA) operated in alternating mode were used to measure nonrefractory submicron aerosol mass and chemical compositions (Jayne et al., 2000; DeCarlo et al., 2006). The average operating time was 1 min for the high-sensitivity V mode and 1 min for high-resolution W mode. The toolkit Squirrel 1.53G was used to analyze time series of various mass components, and Pika 1.12G was used to determine the average element ratios (http://cires1.colorado.edu/jimenez-group/ToFAMSResources/ToFSoftware/index.html). For elemental analysis, the data were analyzed based on the method described in Aiken et al. (2007, 2008). The fragmentation table from Allan et al. (2004) was used to interpret the AMS data. The contribution of gas phase $CO_2$ to the AMS *m/z* 44 signal was corrected by analyzing HEPA filtered air from the smog chamber after filling the exhaust.

**2.4 Operation Steps**

Each experiment consisted of five steps: 1) Introducing exhaust into the chamber from t=-2h. With the injection of exhausts, concentrations of $NO_x$, BC and OA were climbing. Their concentrations when the injection stopped are shown in Table 2. The mixing ratio of $NO_x$ increased from 0 to ~1 ppmv; the particle number concentration increased fast from ~2 to ~350,000 particles $cm^{-3}$; the total particle mass concentrations increased from ~0 to over 100 μg $m^{-3}$; and the VOC concentrations also slightly increased at this step. 2) Characterizing primary emissions from t =−1.5h. After completion of injection, the increase of $NO_x$, BC, OA and VOCs were measured against that of $CO_2$ and CO, and the emission factors were further calculated based on equation (1). 3) Adding HONO and propene at approximately t =−0.5h, leading to a

Atmos. Chem. Phys. Discuss., doi:10.5194/acp-2016-50, 2016
Manuscript under review for journal Atmos. Chem. Phys.
Published: 1 March 2016


moderate increasing of both NO and $NO_2$, approximately 300 ppbv for each. 4) Turning on the lights at t = 0 h to start the photo-oxidation. Substantial amounts of SOA formed at the beginning of this period. 5) Turning off the light at t=5h and further characterizing the aged diesel vehicle exhausts in the dark for about 2 hours.

**2.5 Data analysis**

The emission factors (EF) for various pollutants and the production factors (PF) for SOA were calculated on a fuel basis (g kg-fuel$^{-1}$):

$$EF_P \text{ or } PF_P = 10^3 \cdot [\Delta P]/(\frac{[\Delta CO_2]}{MW_{CO_2}} + \frac{[\Delta CO]}{MW_{CO}}) \cdot \frac{C_f}{MW_C} \qquad (1)$$

Where $[\Delta P]$ is the background corrected pollutant concentration in μg m$^{-3}$, $[\Delta CO_2]$ and $[\Delta \mathrm{CO}]$ is the background corrected concentration of $CO_2$ and CO in the chamber in μg m$^{-3}$. $MW_{CO2}$, $MW_{CO}$ and $MW_C$ are the molecular weights of $CO_2$ (44.1 g mol$^{-1}$), CO (28 g mol$^{-1}$) and carbon (12 g mol$^{-1}$), respectively. $C_f$ is the carbon intensity of the fuel, which was adopted as 0.87 kg C kg-fuel$^{-1}$ for diesel (Chirico et al., 2010). Equation (1) assumes that all carbon in the fuel was converted to $CO_2$ and CO, and the contribution from VOC was negligible. This assumption was reasonable, because $[\Delta CO_2]$ and $[\Delta \mathrm{CO}]$ after introducing exhaust were approximate 100 ppmv and 1 ppmv, respectively, while the increase of VOC was below 5ppbv. The concentrations of hydroxyl radical (OH) during the experiments were inferred from the decay of deuterated butanol measured with the PTR-MS (Atkinson and Arey, 2003). The average OH levels during our experiments were calculated to be approximate 2-5×10$^6$ molecules cm$^{-3}$, which approached to the levels in the ambient and that in the previous study by Gordon et al. (2014b).

Atmos. Chem. Phys. Discuss., doi:10.5194/acp-2016-50, 2016
Manuscript under review for journal Atmos. Chem. Phys.
Published: 1 March 2016


The loss of particles and condensable organic vapors onto the reactor walls need to be corrected to accurately quantify particle concentrations in the smog chamber. In this study, the AMS and SMPS data were corrected for wall loss using the method of Gordon et al. (2014b). Briefly, particulate losses were quantified by assuming that the aerosol was internally mixed and thus, organic aerosol (OA) had the same wall-loss rates with BC. Two limiting cases were considered: ω=0, no organic vapors condense to wall-bound particles; ω=1, organic vapors remain in equilibrium with both wall-bound and suspended particles (Weitkamp et al., 2007).

For ω=0, the loss rate of OA to the chamber wall is

$$\frac{d}{dt}(OA_{wall}) = -k \times OA_{sus} \qquad (2)$$

Where $OA_{wall}$ and $OA_{sus}$ are the wall-bounded and the suspended OA measured at time *t*, respectively, and *k* is the wall loss rate constant of BC.

For ω=1, the total concentration of OA at time *t* ($OA_{total,t}$) was estimated as:

$$OA_{\mathrm{total,t}} = OA_{sus}(t) \times [BC(t_0)/BC(t)] \qquad (3)$$

Where $BC(t_0)$ was the initial BC concentration measured before lights were turned on and $BC(t)$ was the BC concentration after lights were turned on for a time span *t*.

In the experiments with low BC concentrations, we corrected the wall loss effect using exponential fit to the BC data rather than the actual BC data themselves (Gordon et al., 2014b):

$$OM_{WLC} = OM_{Meas}(t)/e^{-kt} \qquad (4)$$

Where *k* is the wall loss rate constant of black carbon.

Atmos. Chem. Phys. Discuss., doi:10.5194/acp-2016-50, 2016
Manuscript under review for journal Atmos. Chem. Phys.
Published: 1 March 2016


Ion enhancement ratios (IER) of the selected ions from the mass spectra of AMS were calculated to evaluate the chemical evolution of POA with aging. The method described by Chirico et al. (2010) is used in this study, and the IER is defined as:

$$\mathrm{IER} = [Ion(t)/Ion(t_0)]/[BC(t)/BC(t_0)] \qquad (5)$$

Where $Ion(t)$ and $Ion(t_0)$ are the ion signals at time $\boldsymbol{t}$ and at the time when the lights were just turned on ($\boldsymbol{t}_0$), respectively.

## 3 Results and discussions

### 3.1 Emission factors of carbonaceous aerosols (BC and POA)

The emission factors of POA and BC are shown in Figure 1. The $EF_{BC}$ were 0.15-0.51 g kg-fuel$^{-1}$ in this study, comparable with those of 0.466-0.763 g kg-fuel$^{-1}$ reported by Chirico et al. (2010) and ~0.260 g kg-fuel$^{-1}$ by Gordon et al. (2014b) at idling condition. Nevertheless, the $EF_{POA}$ (0.18-0.91 g kg-fuel$^{-1}$) were higher than those from previous studies. For instance, the highest emission factors for POA reported by Chirico et al. (2010) were only 0.147 g kg-fuel$^{-1}$. The relatively backward diesel engine technology and lack of emission aftertreatment devices like diesel oxidation catalyst (DOC) or diesel particulate filter (DPF) would probably be the reasons for higher EFs of POA for China's diesel vehicles in this study.

### 3.2 SOA formation from diesel vehicle exhausts

Figure 2 shows the typical temporal evolution of gas and particle phase species during

Atmos. Chem. Phys. Discuss., doi:10.5194/acp-2016-50, 2016
Manuscript under review for journal Atmos. Chem. Phys.
Published: 1 March 2016


a smog chamber experiment (Experiment 8). As showed in Figure 2(c), wall-loss corrected OA started to climb with the formation of SOA after turning on the lights. After 5 h photo-oxidation, the wall loss corrected OA in Experiment 8 increased from 64 μg $m^{-3}$ to 112 μg $m^{-3}$ for ω=0 case and to 166 μg $m^{-3}$ for ω=1 case. However, while the median diameters were increasing with aging (Figure 3(a)), there was no sign of increasing particle numbers, indicating few new particles were formed. Moreover, as shown in Figure 3(b), after about half an hour photo-oxidation (t=0.4), the number of small particles dropped fast, whereas the number concentration of larger particles almost did not change, and the peak diameter slightly increased. It suggested particle growth by coating of the newly formed SOA on existing particles, consistent with the results of Weitkamp et al. (2007).

$PF_{SOA}$ (0.50-1.8 g kg-fuel$^{-1}$) from this study were much higher than those from previous studies, as the highest PF of SOA reported by Chirico et al. (2010) for a medium-duty diesel vehicle (MDDV) at idling condition in Switzerland was merely 0.461 g kg-fuel$^{-1}$. The SOA/POA ratios for all the experiments ranged from 0.6 to 2.4 in this study, lower than that of ~3 for a MDDV at idling condition as reported by Chirico et al. (2010) and the value of approximately 10 for a heavy-duty diesel vehicle (HDDV) at creep condition in the US as reported by Gordon et al. (2014b). Comparatively, the highest $EF_{POA}$ and $PF_{SOA}$ for gasoline vehicle exhaust in China were reported to be 0.0004 g kg-fuel$^{-1}$ and 0.044 g kg-fuel$^{-1}$, respectively (Liu et al., 2015a), which are 1-3 orders of magnitude lower than those for diesel vehicle exhaust according to this study. For this reason, diesel vehicle exhaust would still account for

Atmos. Chem. Phys. Discuss., doi:10.5194/acp-2016-50, 2016
Manuscript under review for journal Atmos. Chem. Phys.
Published: 1 March 2016


a larger portion of traffic-related primary and secondary OA, despite higher faction of gasoline vehicles (83.5%) against that of diesel vehicles (15.2%) in China (MEPC, 2014). As reported in *China Energy Statistical Yearbook* (2013), the fuel consumption of diesel and gasoline for transportation is 107.27 and 37.53 million tons in 2012, so with the POA emission factors and SOA production factors available in this study and in a previous study for gasoline exhaust (Liu et al., 2015a), the diesel derived OA would dominate overwhelmingly over the gasoline derived OA in the traffic-related OA.

### 3.3 SOA yield from precursor VOCs

Aromatic hydrocarbons were considered as very important anthropogenic SOA precursors (Odum et al., 1997). For gasoline vehicle exhaust, aromatics account for 51-90% of formed SOA (Nordin et al., 2013; Liu et al., 2015a). SOA production from aromatics, including benzene, toluene, $C_2$-benzene, $C_2$-benzene, $C_4$-benzene, was estimated by the following formula:

$$\mathrm{SOA_{predicted}} = \sum_i \Delta X_i \times Y_i \qquad (6)$$

Where $\mathrm{SOA_{predicted}}$ (μg $m^{-3}$) is the predicted SOA concentration from precursor *i*; $\Delta X_i$ (μg $m^{-3}$) is the mass of the reacted precursor *i* which was inferred from PRT-ToF-MS data; and $Y_i$ (%) is the SOA yield of precursor *i*. In this study, SOA yields for benzene, toluene, and m-xylene were estimated using the two-product model curves taken from Ng et al. (2007) and those for $C_3$-benzene and $C_4$-benzene were taken from Odum et

Atmos. Chem. Phys. Discuss., doi:10.5194/acp-2016-50, 2016
Manuscript under review for journal Atmos. Chem. Phys.
Published: 1 March 2016


al. (1997).

As presented in Table 3, the predicted SOA concentrations from traditional aromatic precursors accounted for less than 3% of the observed SOA production. Similarly, Weitkamp et al. (2007) reported that SOA formed from 58 known precursors, including aromatics, alkanes and alkenes, just explained less than 8% of the new particle mass in diesel exhaust simulation. It demonstrated that traditional VOC precursors could not explain the amount of diesel SOA formation. One possible reason is that the yields of aromatic hydrocarbons in complex mixture condition might be higher than those in single precursor condition (Song et al, 2007a), thus the SOA mass was probably underestimated. However, even if we took a higher aromatics yield, such as the effective SOA yield of ~30% reported by Gordon et al. (2014b), the discrepancies between predicted and measured SOA were still huge. The unexplained part is probably from the photo-oxidation of the intermediate volatile organic compounds (IVOCs) (Weitkamp et al., 2007; Robinson et al., 2007), such as $C_{13}$-$C_{20}$ *n*-alkanes (Miracolo et al., 2010).

It worth noting that there would be other oxygenated species, like glyoxal and methyl glyoxal, were considered as potential SOA precursors (Volkamer et al., 2006; Carlton et al., 2007; Fu et al., 2008; Kamens et al., 2011). Glyoxal and methyl glyoxal can be primarily emitted from vehicles (Zhang et al., 2016), or secondarily formed by the photo-oxidation of VOCs (Carlton et al., 2007; Healy et al., 2008; Volkamer et al., 2009). The PTR-ToF-MS measured ion *m/z* 59 represents acetone and glyoxal, and

Atmos. Chem. Phys. Discuss., doi:10.5194/acp-2016-50, 2016
Manuscript under review for journal Atmos. Chem. Phys.
Published: 1 March 2016


ion *m/z* 73 represents methyl glyoxal (Healy et al., 2008; Kahnt et al., 2011). The evolution of *m/z* 59 and *m/z* 73 was shown in Figure 4. When we introduced diesel vehicle exhaust, the mixing ratios of *m/z* 59 and *m/z* 73 increased from ~0 to 11 and to 2.5 ppbv, respectively; after 5 hours photo-oxidation, the mixing ratios of *m/z* 59 and *m/z* 73 further increased to 71 and 6.0 ppbv, indicating secondary formation of glyoxal and methyl glyoxal during photo-oxidation. Therefore, the primary and secondary glyoxal and methyl glyoxal could also partly explain the SOA formation from diesel vehicle exhaust.

### 3.4 Chemical evolution of OA

Figure 5 showed the average AMS mass spectra for the total OA measured in the beginning and at the end of a typical simulation (Experiment 8). According to the method described by Chirico et al. (2010), high resolution mass spectra was divided into 4 organic fragment classes, namely CH, CHO (including fragments only with C and O), CHN and CHON.

Very similar to those in previous studies (Weitkamp et al., 2007; Chirico et al., 2010; Presto et al., 2014), POA spectra in the beginning were dominated by the $C_nH_{2n+1}^+$ organic fragment ion group (*m/z* 29, 43, 57, 71,…) characteristic of alkanes (Figure 5(a)). They also had a prominent $C_nH_{2n-1}^+$ sequence (*m/z* 27, 41, 55, 69,…) that is associated with cycloalkanes and alkenes (Canagaratna et al., 2004). The POA from all the experiment show that the largest signal contribution is from *m/z* 43 (47% of which is $C_3H_7^+$, and 52% of which is $C_2H_3O^+$), followed by *m/z* 41 (97 % of which is

Atmos. Chem. Phys. Discuss., doi:10.5194/acp-2016-50, 2016
Manuscript under review for journal Atmos. Chem. Phys.
Published: 1 March 2016


$C_3H_5^+$ ). A certain amount of signals for PAHs, such as *m/z* 128 for naphthalene, 152 for acenaphthylene, 178 for phenanthrene or anthracene and 202 for fluoranthene or pyrene, were also observed, and the fractions of these fragments in total OA signal were 0.5%, 0.3%, 0.2% and 0.1%, respectively. Overall, In the beginning CH class took the largest fraction of approximate 67.6% in total OA, followed by the CHO class (29.2%), while the fractions of CHN (1.8%) and CHON (1.4%) class were much lower. Compared with the distribution pattern (75.2% for CH and 22.8% for CHO) reported by Chirico et al. (2010), POA spectra in this study had a lower CH class but higher CHO class, suggesting more oxidized components in the initially emitted exhausts.

The aged OA mass spectrum shown in Figure 5(b) is averaged over the last one hour of the experiment. After 5-hour aging, the contribution to total organic mass by fragments *m/z* 44, representing oxidized organics with ~98% of which consisted of $CO_2^+$ and $C_2H_4O^+$, increased from 5.6% to 10.6%. Meanwhile, the signal of *m/z* 57, which generally associated with primary emissions (Weitkamp et al., 2007; Sage et al., 2008), dropped form 3.7% to 2.2%. Moreover, the fraction of $C_3H_7^+$ in *m/z* 43 decreased drastically from 47% to 17%, whereas the fraction of $C_2H_3O^+$ in *m/z* 43 increased from 55% to 81%. The relative contribution of the ion classes also changed significantly after 5 hours photo-oxidation compared to those of POA. The fraction of CH class fell from 67.6% to 48.3%, whereas that of the CHO class grew from 29.2% to 47.6%, indicating a more oxidized chemical property. The CHN and CHON classes contributed 2.3% and 1.7%, respectively; they were also minor components although

Atmos. Chem. Phys. Discuss., doi:10.5194/acp-2016-50, 2016
Manuscript under review for journal Atmos. Chem. Phys.
Published: 1 March 2016


their factions were becoming higher.

Figure 6 presents typical temporal evolutions of the H/C and O/C atomic ratios as well as the OM/OC ratio measured by the AMS (Experiment 8). With photo-oxidation, the average ratios for O/C and OM/OC slightly increased from 0.26 to 0.47 and from 1.48 to 1.76, respectively; while that for H/C ratio decreased from 1.50 to 1.43. The increase of O/C and OM/OC ratios and decrease of H/C ratios after photo-oxidation were found during all the experiments (Table 2), further confirming the increased oxidation state of OA during aging. It should be pointed out that the increase of oxidation state is due to not only the formation of SOA, but also further oxidation or degradation of POA. For example, as shown in Figure 7, the IERs of polycyclic aromatic hydrocarbons (PAHs) signals such as $C_{10}H_8^+$, $C_{12}H_8^+$, $C_{14}H_{10}^+$, $C_{16}H_{10}^+$, which represent naphthalene, acenaphthylene, phenanthrene or anthracene, fluoranthene or pyrene, respectively, decreased substantially after 5-hour aging. It indicates that PAHs, probably along with other POA species, were oxidized through heterogeneous reaction, or vaporized to gas phase, oxidized and then condensed back onto particles (Donahue et al., 2006; Robinson et al., 2007).

The $f_{43}$ versus $f_{44}$ triangle plot for OA in our experiments is presented in Figure 8(a). Compared with POA, SOA had higher $f_{44}$ and lower $f_{43}$ values. According to Ng et al. (2010), ambient low-volatility oxygenated OA (LV-OOA) and SV-OOA factors fall in the upper and lower portions of the triangle, respectively. Similar with that reported by Presto et al. (2014) for diesel SOA, the plots of SOA were within the range of

SV-OOA. Figure 8(b) translates the AMS data into van Krevelen space. The van Krevelen slopes for this study ranged from -0.47 to -0.68, which were similar to that reported by Presto et al. (2014) for diesel exhaust experiments, and also in the range of slopes for ambient OOA factors observed by Ng et al. (2011). It indicates that the SOA chemistry observed in present smog chamber experiments is atmospherically relevant (Presto et al., 2014). According to Heald et al. (2010) and Ng et al. (2011), slopes of -1 and 0 in the Van Krevelen diagram represent chemical reaction for addition of carboxylic acid and alcohol/peroxide, respectively. Therefore, the van Krevelen slopes in this study suggest that SOA formed was a combination of carboxylic acids and alcohols/peroxides.

## 4 Conclusions

In this paper, chamber simulations were conducted to investigate SOA formation from diluted exhaust of three types of diesel vehicles widely used in China. $EF_{POA}$ and $PF_{SOA}$ in this work were 0.19 and 0.61 g kg-fuel$^{-1}$ for JAC, 0.18-0.34 and 0.56-0.76 g kg-fuel$^{-1}$ for Foton, 0.72-0.91 and 0.50-1.8 g kg-fuel$^{-1}$ for Changan, respectively, which were all higher than those reported in previous studies in Europe and in the US. These $EF_{POA}$ and $PF_{SOA}$ values were also 2-3 and 1 orders of magnitude higher than those of gasoline vehicle exhaust. Therefore, although diesel vehicle population is much less than that of gasoline in China, it still plays a vital role in the contribution of primary and secondary OA. It should be noted that all the experiments for SOA formation from both gasoline and diesel vehicles in China were conducted under

idling condition. The emission of POA as well as formation SOA under different operating modes, especially on-road conditions, deserves further investigation.

According to our study, less than 3% of diesel SOA production can be explained by aromatics, consistent with previous diesel exhaust studies. It demonstrated that there existed substantial unknown precursors. Photo-oxidation of high molecular weight hydrocarbons including IVOCs and PAHs, as well as heterogeneous reaction of oxygenated species like glyoxal and methyl glyoxal, might contribute to the SOA formation from diesel vehicle exhausts. SOA from diesel vehicles belongs to SV-OOA based on AMS data. The van Krevelen slopes in our experiments were between -0.47 and -0.68, suggesting that SOA formed is a combination of carboxylic acids and alcohols/peroxides.

## Acknowledgments

This study was supported by the Strategic Priority Research Program of the Chinese Academy of Sciences (XDB05010200), the National Natural Science Foundation of China (41025012/41571130031).

## References

Aiken, A. C., DeCarlo, P. F., and Jimenez, J. L.: Elemental analysis of organic species with electron ionization high-resolution mass spectrometry, Anal. Chem., 79, 8350-8358, doi:10.1021/ac071150w, 2007.

Aiken, A. C., DeCarlo, P. F., Kroll, J. H., Worsnop, D. R., Huffman, J. A., Docherty, K. S., Ulbrich, I. M., Mohr, C., Kimmel, J. R., Sueper, D., Sun, Y., Zhang, Q.,

Trimborn, A., Northway, M., Ziemann, P. J., Canagaratna, M. R., Onasch, T. B., Alfarra, M. R., Prevot, A. S. H., Dommen, J., Duplissy, J., Metzger, A., Baltensperger, U., and Jimenez, J. L.: O/C and OM/OC ratios of primary, secondary, and ambient organic aerosols with high-resolution time-of-flight aerosol mass spectrometry, Environ. Sci. Technol., 42, 4478-4485, doi:10.1021/es703009q, 2008.

Allan, J. D., Delia, A. E., Coe, H., Bower, K. N., Alfarra, M. R., Jimenez, J. L., Middlebrook, A. M., Drewnick, F., Onasch, T. B., Canagaratna, M. R., Jayne, J. T., and Worsnop, D. R.: A generalised method for the extraction of chemically resolved mass spectra from aerodyne aerosol mass spectrometer data, Int. J. Mass Spectrom. Ion Processes, 35, 909-922, doi:10.1016/j.jaerosci.2004.02.007, 2004.

Atkinson, R., and Arey, J.: Atmospheric degradation of volatile organic compounds, Chem. Rev., 103, 4605-4638, doi:10.1021/cr0206420, 2003.

Barmet, P., Dommen, J., DeCarlo, P. F., Tritscher, T., Praplan, A. P., Platt, S. M., Prevot, A. S. H., Donahue, N. M., and Baltensperger, U.: OH clock determination by proton transfer reaction mass spectrometry at an environmental chamber, Atmos. Meas. Tech., 5, 647-656, doi:10.5194/amt-5-647-2012, 2012.

Brook, R. D., Rajagopalan, S., Pope, C. A., 3rd, Brook, J. R., Bhatnagar, A., Diez-Roux, A. V., Holguin, F., Hong, Y., Luepker, R. V., Mittleman, M. A., Peters, A., Siscovick, D., Smith, S. C., Jr., Whitsel, L., Kaufman, J. D., and on behalf of the American Heart Association Council On Epidemiology and Prevention, Council on the Kidney in Cardiovascular Disease, Council on Nutrition, Physical Activity and Metabolism: Particulate matter air pollution and cardiovascular disease: An

update to the scientific statement from the American Heart Association, Circulation, 121, 2331-2378, doi:10.1161/CIR.0b013e3181dbece1, 2010.

Canagaratna, M. R., Jayne, J. T., Ghertner, D. A., Herndon, S., Shi, Q., Jimenez, J. L., Silva, P. J., Williams, P., Lanni, T., Drewnick, F., Demerjian, K. L., Kolb, C. E., and Worsnop, D. R.: Chase studies of particulate emissions from in-use New York City vehicles, Aerosol Sci. Technol., 38, 555-573, doi:10.1080/02786820490465504, 2004.

Carlton, A. G., Turpin, B. J., Altieri, K. E., Seitzinger, S., Reff, A., Lim, H.-J., and Ervens, B.: Atmospheric oxalic acid and SOA production from glyoxal: Results of aqueous photooxidation experiments, Atmos. Environ., 41, 7588-7602, doi:10.1016/j.atmosenv.2007.05.035, 2007.

Chen, Y., Zheng, M., Edgerton, E. S., Ke, L., Sheng, G., and Fu, J.: $PM_{2.5}$ source apportionment in the southeastern U.S.: Spatial and seasonal variations during 2001–2005, J. Geophys. Res., 117, D08304, doi:10.1029/2011JD016572, 2012.

Cheung, K. L., Polidori, A., Ntziachristos, L., Tzamkiozis, T., Samaras, Z., Cassee, F. R., Gerlofs, M., and Sioutas, C.: Chemical characteristics and oxidative potential of particulate matter emissions from gasoline, diesel, and biodiesel cars, Environ. Sci. Technol., 43, 6334-6340, doi:10.1021/es900819t, 2009.

China Association of Automobile Manufactures, China Automotive Industry Yearbook 2011, 2012.

Chirico, R., DeCarlo, P. F., Heringa, M. F., Tritscher, T., Richter, R., Prevot, A. S. H., Dommen, J., Weingartner, E., Wehrle, G., Gysel, M., Laborde, M., and

Baltensperger, U.: Impact of aftertreatment devices on primary emissions and secondary organic aerosol formation potential from in-use diesel vehicles: results from smog chamber experiments, Atmos. Chem. Phys., 10, 11545-11563, doi:10.5194/acp-10-11545-2010, 2010.

Cocker, D. R., Mader, B. T., Kalberer, M., Flagan, R. C., and Seinfeld, J. H.: The effect of water on gas-particle partitioning of secondary organic aerosol: II. m-xylene and 1,3,5-trimethylbenzene photooxidation systems, Atmos. Environ., 35, 6073-6085, doi:10.1016/s1352-2310(01)00405-8, 2001.

Cui, H., Chen, W., Dai, W., Liu, H., Wang, X., and He, K.: Source apportionment of $PM_{2.5}$ in Guangzhou combining observation data analysis and chemical transport model simulation, Atmos. Environ., 116, 262-271, doi:10.1016/j.atmosenv.2015.06.054, 2015.

DeCarlo, P. F., Kimmel, J. R., Trimborn, A., Northway, M. J., Jayne, J. T., Aiken, A. C., Gonin, M., Fuhrer, K., Horvath, T., Docherty, K. S., Worsnop, D. R., and Jimenez, J. L.: Field-deployable, high-resolution, time-of-flight aerosol mass spectrometer, Anal. Chem., 78, 8281-8289, doi:10.1021/ac061249n, 2006.

Donahue, N. M., Robinson, A. L., Stanier, C. O., and Pandis, S. N.: Coupled partitioning, dilution, and chemical aging of semivolatile organics, Environ. Sci. Technol., 40, 2635-2643, doi:10.1021/es052297c, 2006.

Fu, T.-M., Jacob, D. J., Wittrock, F., Burrows, J. P., Vrekoussis, M., and Henze, D. K.: Global budgets of atmospheric glyoxal and methylglyoxal, and implications for formation of secondary organic aerosols, J. Geophys. Res., 113, D15303,

doi:10.1029/2007JD009505, 2008.

Gordon, T. D., Presto, A. A., May, A. A., Nguyen, N. T., Lipsky, E. M., Donahue, N. M., Gutierrez, A., Zhang, M., Maddox, C., Rieger, P., Chattopadhyay, S., Maldonado, H., Maricq, M. M., and Robinson, A. L.: Secondary organic aerosol formation exceeds primary particulate matter emissions for light-duty gasoline vehicles, Atmos. Chem. Phys., 14, 4661-4678, doi:10.5194/acp-14-4661-2014, 2014a.

Gordon, T. D., Presto, A. A., Nguyen, N. T., Robertson, W. H., Na, K., Sahay, K. N., Zhang, M., Maddox, C., Rieger, P., Chattopadhyay, S., Maldonado, H., Maricq, M. M., and Robinson, A. L.: Secondary organic aerosol production from diesel vehicle exhaust: impact of aftertreatment, fuel chemistry and driving cycle, Atmos. Chem. Phys., 14, 4643-4659, doi:10.5194/acp-14-4643-2014, 2014b.

Guo, S., Hu, M., Zamora, M. L., Peng, J., Shang, D., Zheng, J., Du, Z., Wu, Z., Shao, M., Zeng, L., Molina, M. J., and Zhang, R.: Elucidating severe urban haze formation in China, Proc. Natl. Acad. Sci. USA, 111, 17373-17378, doi:10.1073/pnas.1419604111, 2014.

Heald, C. L., Kroll, J. H., Jimenez, J. L., Docherty, K. S., DeCarlo, P. F., Aiken, A. C., Chen, Q., Martin, S. T., Farmer, D. K., and Artaxo, P.: A simplified description of the evolution of organic aerosol composition in the atmosphere, Geophys. Res. Lett., 37, L08803, doi:10.1029/2010GL042737, 2010.

Healy, R. M., Wenger, J. C., Metzger, A., Duplissy, J., Kalberer, M., and Dommen, J.: Gas/particle partitioning of carbonyls in the photooxidation of isoprene and

1,3,5-trimethylbenzene, Atmos. Chem. Phys., 8, 3215-3230, 2008.

Huang, R. J., Zhang, Y., Bozzetti, C., Ho, K. F., Cao, J. J., Han, Y., Daellenbach, K. R., Slowik, J. G., Platt, S. M., Canonaco, F., Zotter, P., Wolf, R., Pieber, S. M., Bruns, E. A., Crippa, M., Ciarelli, G., Piazzalunga, A., Schwikowski, M., Abbaszade, G., Schnelle-Kreis, J., Zimmermann, R., An, Z., Szidat, S., Baltensperger, U., El Haddad, I., and Prevot, A. S.: High secondary aerosol contribution to particulate pollution during haze events in China, Nature, 514, 218-222, doi:10.1038/nature13774, 2014.

Jathar, S. H., Gordon, T. D., Hennigan, C. J., Pye, H. O., Pouliot, G., Adams, P. J., Donahue, N. M., and Robinson, A. L.: Unspeciated organic emissions from combustion sources and their influence on the secondary organic aerosol budget in the United States, Proc. Natl. Acad. Sci. USA, 111, 10473-10478, doi:10.1073/pnas.1323740111, 2014.

Jayne, J. T., Leard, D. C., Zhang, X. F., Davidovits, P., Smith, K. A., Kolb, C. E., and Worsnop, D. R.: Development of an aerosol mass spectrometer for size and composition analysis of submicron particles, Aerosol Sci. Technol., 33, 49-70, doi:10.1080/027868200410840, 2000.

Jordan, A., Haidacher, S., Hanel, G., Hartungen, E., Märk, L., Seehauser, H., Schottkowsky, R., Sulzer, P., and Märk, T. D.: A high resolution and high sensitivity proton-transfer-reaction time-of-flight mass spectrometer (PTR-TOF-MS), Int. J. Mass spectrom., 286, 122-128, doi:10.1016/j.ijms.2009.07.005, 2009.

Kahnt, A., Iinuma, Y., Böge, O., Mutzel, A., and Herrmann, H.: Denuder sampling

techniques for the determination of gas-phase carbonyl compounds: A comparison and characterisation of in situ and ex situ derivatisation methods, J. Chromatogr. B, 879, 1402-1411, doi:10.1016/j.jchromb.2011.02.028, 2011.

Kamens, R. M., Zhang, H., Chen, E. H., Zhou, Y., Parikh, H. M., Wilson, R. L., Galloway, K. E., and Rosen, E. P.: Secondary organic aerosol formation from toluene in an atmospheric hydrocarbon mixture: Water and particle seed effects, Atmos. Environ., 45, 2324-2334, doi:10.1016/j.atmosenv.2010.11.007, 2011.

Kirchstetter, T. W., and Novakov, T.: Controlled generation of black carbon particles from a diffusion flame and applications in evaluating black carbon measurement methods, Atmos. Environ., 41, 1874-1888, doi:10.1016/j.atmosenv.2006.10.067, 2007.

Lelieveld, J., Evans, J. S., Fnais, M., Giannadaki, D., and Pozzer, A.: The contribution of outdoor air pollution sources to premature mortality on a global scale, Nature, 525, 367-371, doi:10.1038/nature15371, 2015.

Lindinger, W., Hansel, A., and Jordan, A.: On-line monitoring of volatile organic compounds at pptv levels by means of proton-transfer-reaction mass spectrometry (PTR-MS) medical applications, food control and environmental research, Int. J. Mass Spectrom. Ion Processes, 173, 191-241, doi:10.1016/S0168-1176(97)00281-4, 1998.

Liu, H., He, K., Lents, J. M., Wang, Q., and Tolvett, S.: Characteristics of diesel truck emission in China based on portable emissions measurement systems, Environ. Sci. Technol., 43, 9507-9511, doi:10.1021/es902044x, 2009.

Liu, T., Wang, X., Deng, W., Hu, Q., Ding, X., Zhang, Y., He, Q., Zhang, Z., Lü, S., Bi, X., Chen, J., and Yu, J.: Secondary organic aerosol formation from photochemical aging of light-duty gasoline vehicle exhausts in a smog chamber, Atmos. Chem. Phys., 15, 9049-9062, doi:10.5194/acp-15-9049-2015, 2015a.

Liu, Z., Guan, D., Wei, W., Davis, S. J., Ciais, P., Bai, J., Peng, S., Zhang, Q., Hubacek, K., Marland, G., Andres, R. J., Crawford-Brown, D., Lin, J., Zhao, H., Hong, C., Boden, T. A., Feng, K., Peters, G. P., Xi, F., Liu, J., Li, Y., Zhao, Y., Zeng, N., and He, K.: Reduced carbon emission estimates from fossil fuel combustion and cement production in China, Nature, 524, 335-338, doi:10.1038/nature14677, 2015b.

Ministry of Environmental Protection of China (MEPC). China Vehicle Emission Control Annual Report 2014. 2015.

Miracolo, M. A., Presto, A. A., Lambe, A. T., Hennigan, C. J., Donahue, N. M., Kroll, J. H., Worsnop, D. R., and Robinson, A. L.: Photo-oxidation of low-volatility organics found in motor vehicle emissions: Production and chemical evolution of organic aerosol mass, Environ. Sci. Technol., 44, 1638-1643, doi:10.1021/es902635c, 2010.

National Bureau of Statistics of China, Energy Statistics Division. China Energy Statistical Yearbook 2013, 2014.

Ng, N. L., Kroll, J. H., Chan, A. W. H., Chhabra, P. S., Flagan, R. C., and Seinfeld, J. H.: Secondary organic aerosol formation from m-xylene, toluene, and benzene, Atmos. Chem. Phys., 7, 3909-3922, doi:10.5194/acp-7-3909-2007, 2007.

Ng, N. L., Canagaratna, M. R., Zhang, Q., Jimenez, J. L., Tian, J., Ulbrich, I. M., Kroll, J. H., Docherty, K. S., Chhabra, P. S., Bahreini, R., Murphy, S. M., Seinfeld, J. H., Hildebrandt, L., Donahue, N. M., DeCarlo, P. F., Lanz, V. A., Prévôt, A. S. H., Dinar, E., Rudich, Y., and Worsnop, D. R.: Organic aerosol components observed in Northern hemispheric datasets from aerosol mass spectrometry, Atmos. Chem. Phys., 10, 4625-4641, doi:10.5194/acp-10-4625-2010, 2010.

Ng, N. L., Canagaratna, M. R., Jimenez, J. L., Chhabra, P. S., Seinfeld, J. H., and Worsnop, D. R.: Changes in organic aerosol composition with aging inferred from aerosol mass spectra, Atmos. Chem. Phys., 11, 6465-6474, doi:10.5194/acp-11-6465-2011, 2011.

Nordin, E. Z., Eriksson, A. C., Roldin, P., Nilsson, P. T., Carlsson, J. E., Kajos, M. K., Hellén, H., Wittbom, C., Rissler, J., Löndahl, J., Swietlicki, E., Svenningsson, B., Bohgard, M., Kulmala, M., Hallquist, M., and Pagels, J. H.: Secondary organic aerosol formation from idling gasoline passenger vehicle emissions investigated in a smog chamber, Atmos. Chem. Phys., 13, 6101-6116, doi:10.5194/acp-13-6101-2013, 2013.

Odum, J. R., Hoffmann, T., Bowman, F., Collins, D., Flagan, R. C., and Seinfeld, J. H.: Gas/particle partitioning and secondary organic aerosol yields, Environ. Sci. Technol., 30, 2580-2585, doi:10.1021/es950943+, 1996.

Odum, J. R., Jungkamp, T. P. W., Griffin, R. J., Flagan, R. C., and Seinfeld, J. H.: The atmospheric aerosol-forming potential of whole gasoline vapor, Science, 276, 96-99, doi:10.1126/science.276.5309.96, 1997.

Parrish, D. D., and Zhu, T.: Clean Air for Megacities, Science, 326, 674-675, doi:10.1126/science.1176064, 2009.

Pope, C. A., Ezzati, M., and Dockery, D. W.: Fine-particulate air pollution and life expectancy in the United States, N. Engl. J. Med., 360, 376-386, doi:10.1056/NEJMsa0805646, 2009.

Presto, A. A., Gordon, T. D., and Robinson, A. L.: Primary to secondary organic aerosol: evolution of organic emissions from mobile combustion sources, Atmos. Chem. Phys., 14, 5015-5036, doi:10.5194/acp-14-5015-2014, 2014.

Ramanathan, V., Crutzen, P. J., Kiehl, J. T., and Rosenfeld, D.: Aerosols, climate, and the hydrological cycle, Science, 294, 2119-2124, doi:10.1126/science.1064034, 2001.

Reff, A., Bhave, P. V., Simon, H., Pace, T. G., Pouliot, G. A., Mobley, J. D., and Houyoux, M.: Emissions inventory of $PM_{2.5}$ trace elements across the United States, Environ. Sci. Technol., 43, 5790-5796, doi:10.1021/es802930x, 2009.

Robinson, A. L., Donahue, N. M., Shrivastava, M. K., Weitkamp, E. A., Sage, A. M., Grieshop, A. P., Lane, T. E., Pierce, J. R., and Pandis, S. N.: Rethinking organic aerosols: semivolatile emissions and photochemical aging, Science, 315, 1259-1262, doi:10.1126/science.1133061, 2007.

Sage, A. M., Weitkamp, E. A., Robinson, A. L., and Donahue, N. M.: Evolving mass spectra of the oxidized component of organic aerosol: results from aerosol mass spectrometer analyses of aged diesel emissions, Atmos. Chem. Phys., 8, 1139-1152, 2008.

Song, C., Na, K., Warren, B., Malloy, Q., and Cocker, D. R., III: Impact of propene on secondary organic aerosol formation from m-xylene, Environ. Sci. Technol., 41, 6990-6995, doi:10.1021/es062279a, 2007a.

Song, Y., Xie, S., Zhang, Y., Zeng, L., Salmon, L. G., and Zheng, M.: Source apportionment of $PM_{2.5}$ in Beijing using principal component analysis/absolute principal component scores and UNMIX, Sci. Total Environ., 372, 278-286, doi:10.1016/j.scitotenv.2006.08.041, 2006a.

Song, Y., Zhang, Y. H., Xie, S. D., Zeng, L. M., Zheng, M., Salmon, L. G., Shao, M., and Slanina, S.: Source apportionment of $PM_{2.5}$ in Beijing by positive matrix factorization, Atmos. Environ., 40, 1526-1537, doi:10.1016/j.atmosenv.2005.10.039, 2006b.

Song, Y., Tang, X., Xie, S., Zhang, Y., Wei, Y., Zhang, M., Zeng, L., and Lu, S.: Source apportionment of $PM_{2.5}$ in Beijing in 2004, J. Hazard. Mater., 146, 124-130, doi:10.1016/j.jhazmat.2006.11.058, 2007b.

Stone, E. A., Snyder, D. C., Sheesley, R. J., Sullivan, A. P., Weber, R. J., and Schauer, J. J.: Source apportionment of fine organic aerosol in Mexico City during the MILAGRO experiment 2006, Atmos. Chem. Phys., 8, 1249-1259, doi:10.5194/acp-8-1249-2008, 2008.

Volkamer, R., Jimenez, J. L., San Martini, F., Dzepina, K., Zhang, Q., Salcedo, D., Molina, L. T., Worsnop, D. R., and Molina, M. J.: Secondary organic aerosol formation from anthropogenic air pollution: Rapid and higher than expected, Geophys. Res. Lett., 33, L17811, doi:10.1029/2006GL026899, 2006.

Volkamer, R., Ziemann, P. J., and Molina, M. J.: Secondary Organic Aerosol Formation from Acetylene ($C_2H_2$): seed effect on SOA yields due to organic photochemistry in the aerosol aqueous phase, Atmos. Chem. Phys., 9, 1907-1928, 2009.

Wang, H., Fu, L., Zhou, Y., Du, X., and Ge, W.: Trends in vehicular emissions in China's mega cities from 1995 to 2005, Environ. Pollut., 158, 394-400, doi:10.1016/j.envpol.2009.09.002, 2010.

Wang, X., Liu, T., Bernard, F., Ding, X., Wen, S., Zhang, Y., Zhang, Z., He, Q., Lu, S., Chen, J., Saunders, S., and Yu, J.: Design and characterization of a smog chamber for studying gas-phase chemical mechanisms and aerosol formation, Atmos. Meas. Tech., 7, 301-313, doi:10.5194/amt-7-301-2014, 2014a.

Wang, Y., Wang, M., Zhang, R., Ghan, S. J., Lin, Y., Hu, J., Pan, B., Levy, M., Jiang, J. H., and Molina, M. J.: Assessing the effects of anthropogenic aerosols on Pacific storm track using a multiscale global climate model, Proc. Natl. Acad. Sci. USA, 111, 6894-6899, doi:10.1073/pnas.1403364111, 2014b.

Weitkamp, E. A., Sage, A. M., Pierce, J. R., Donahue, N. M., and Robinson, A. L.: Organic aerosol formation from photochemical oxidation of diesel exhaust in a smog chamber, Environ. Sci. Technol., 41, 6969-6975, doi:10.1021/es070193r, 2007.

Wu, S., Deng, F., Wei, H., Huang, J., Wang, X., Hao, Y., Zheng, C., Qin, Y., Lv, H., Shima, M., and Guo, X.: Association of cardiopulmonary health effects with source-appointed ambient fine particulate in Beijing, China: a combined analysis

from the Healthy Volunteer Natural Relocation (HVNR) study, Environ. Sci. Technol., 48, 3438-3448, doi:10.1021/es404778w, 2014.

Xu, H., Wang, X., Pöschl, U., Feng, S., Wu, D., Yang, L., Li, S., Song, W., Sheng, G., Fu, J.: Genotoxicity of total and fractionated extractable organic matter in fine air particulate matter in urban Guangzhou: comparison between haze and nonhaze episodes, Environ. Toxicol. Chem., 27, 206-212, doi:10.1897/07-095.1, 2008.

Yanowitz, J., McCormick, R. L., and Graboski, M. S.: In-use emissions from heavy-duty diesel vehicles, Environ. Sci. Technol., 34, 729-740, doi:10.1021/es990903w, 2000.

Yi, Z., Wang, X., Sheng, G., Zhang, D., Zhou, G., and Fu, J.: Soil uptake of carbonyl sulfide in subtropical forests with different successional stages in south China, J. Geophys. Res., 112, D08302, doi:10.1029/2006JD008048, 2007.

Zhang, Q., Streets, D. G., Carmichael, G. R., He, K. B., Huo, H., Kannari, A., Klimont, Z., Park, I. S., Reddy, S., Fu, J. S., Chen, D., Duan, L., Lei, Y., Wang, L. T., and Yao, Z. L.: Asian emissions in 2006 for the NASA INTEX-B mission, Atmos. Chem. Phys., 9, 5131-5153, 2009.

Zhang, R., Jing, J., Tao, J., Hsu, S. C., Wang, G., Cao, J., Lee, C. S. L., Zhu, L., Chen, Z., Zhao, Y., and Shen, Z.: Chemical characterization and source apportionment of $PM_{2.5}$ in Beijing: seasonal perspective, Atmos. Chem. Phys., 13, 7053-7074, doi:10.5194/acp-13-7053-2013, 2013.

Zhang, Y., Wang, X., Blake, D. R., Li, L., Zhang, Z., Wang, S., Guo, H., Lee, F. S. C., Gao, B., Chan, L., Wu, D., and Rowland, F. S.: Aromatic hydrocarbons as ozone

precursors before and after outbreak of the 2008 financial crisis in the Pearl River Delta region, south China, J. Geophys. Res., 117, D15306, doi:10.1029/2011JD017356, 2012.

Zhang, Y., Wang, X., Wen, S., Herrmann, H., Yang, W., Huang, X., Zhang, Z., Huang, Z., He, Q., and George, C.: On-road vehicle emissions of glyoxal and methylglyoxal from tunnel tests in urban Guangzhou, China, Atmos. Environ., 127, 55-60, doi:10.1016/j.atmosenv.2015.12.017, 2016.

Zhao, L., Wang, X., He, Q., Wang, H., Sheng, G., Chan, L., Fu, J., Blake, D.R: Exposure to hazardous volatile organic compounds, $PM_{10}$ and CO while walking along streets in urban Guangzhou, China, Atmo. Environ., 38, 6177-6184, doi:10.1016/j.atmosenv.2004.07.025, 2004

Zheng, M., Salmon, L. G., Schauer, J. J., Zeng, L. M., Kiang, C. S., Zhang, Y. H., and Cass, G. R.: Seasonal trends in $PM_{2.5}$ source contributions in Beijing, China, Atmos. Environ., 39, 3967-3976, doi:10.1016/j.atmosenv.2005.03.036, 2005.

Atmos. Chem. Phys. Discuss., doi:10.5194/acp-2016-50, 2016
Manuscript under review for journal Atmos. Chem. Phys.
Published: 1 March 2016


**Table 1** Information of three diesel vehicles used in the experiments

| | Vehicle ID | Emission standard | Model year | Mileage (km) | Displacement ($cm^{-3}$) | Power (kW) | Weight (kg) |
|---|---|---|---|---|---|---|---|
| MDDV | Foton | Euro III | 2011 | 16,000 | 2,499 | 65 | 2,580 |
| | Changan | Euro III | 2013 | 15,000 | 2,540 | 67 | 3,775 |
| HDDV | JAC | Euro III | 2013 | 11,000 | 9,839 | 215 | 24,900 |

Atmos. Chem. Phys. Discuss., doi:10.5194/acp-2016-50, 2016
Manuscript under review for journal Atmos. Chem. Phys.
Published: 1 March 2016


**Table 2** Summary of the results for the diesel vehicle experiments

| Experiment | Vehicle | T (℃) | RH (%) | NO [a] (ppbv) | $NO_2$ [a] (ppbv) | OH[b] | $EF_{BC}$ (g $kg^{-1}$ fuel) | $EF_{POA}$ (g $kg^{-1}$ fuel) | $PF_{SOA}$ (g $kg^{-1}$ fuel) | | O/C | | H/C | | OM/OC | |
|---|---|---|---|---|---|---|---|---|---|---|---|---|---|---|---|---|
| | | | | | | | | | ω=0 | ω=1 | ini[c] | fin[d] | ini[c] | fin[d] | ini[c] | fin[d] |
| 1 | JAC | 24.2 | 2.3 | 3246 | 220 | 3.11 | 0.16 | 0.19 | 0.30 | 0.61 | 0.65 | 0.86 | 1.36 | 1.21 | 2.01 | 2.29 |
| 2 | Foton | 24.9 | 2.5 | 1156 | 144 | 1.74 | 0.19 | 0.34 | 0.26 | 0.56 | 0.11 | 0.17 | 1.81 | 1.71 | 1.33 | 1.40 |
| 3 | Foton | 24.1 | 1.5 | 1185 | 136 | 5.23 | 0.18 | 0.28 | 0.28 | 0.68 | 0.16 | 0.30 | 1.70 | 1.62 | 1.36 | 1.55 |
| 4 | Foton | 24.9 | 2.7 | 749 | 153 | 5.00 | 0.19 | 0.32 | 0.34 | 0.76 | 0.69 | 0.80 | 1.37 | 1.23 | 2.14 | 2.25 |
| 5 | Foton | 25.2 | 54 | 2151 | 236 | 2.24 | 0.15 | 0.18 | 0.23 | 0.60 | 0.37 | 0.68 | 1.53 | 1.31 | 1.64 | 2.04 |
| 6 | Changan | 24.7 | 2.5 | 733 | 248 | 3.99 | 0.47 | 0.91 | 0.62 | 1.8 | 0.50 | 0.66 | 1.40 | 1.37 | 1.80 | 2.02 |
| 7 | Changan | 24.5 | 1.7 | 1113 | 43 | 4.23 | 0.50 | 0.74 | 0.39 | 0.50 | 0.34 | 0.51 | 1.41 | 1.39 | 1.75 | 1.82 |
| 8 | Changan | 24.6 | 54 | 1286 | 205 | 4.10 | 0.51 | 0.72 | 0.57 | 1.1 | 0.26 | 0.47 | 1.51 | 1.43 | 1.48 | 1.76 |

[a]. before adding HONO.
[b]. $\times 10^6$ molecules $cm^{-3}$
[c]. initial value, the value before turned on the lights.
[d]. final value, the value after 5 hours photo-oxidation.

Atmos. Chem. Phys. Discuss., doi:10.5194/acp-2016-50, 2016
Manuscript under review for journal Atmos. Chem. Phys.
Published: 1 March 2016


**Table 3** The predicted SOA production from each aromatic hydrocarbons (measured by PTR-MS) in all experiments.

| Experiment | Predicted SOA (μg $m^{-3}$) | | | | | Predicted SOA/ Measured SOA [a] |
|---|---|---|---|---|---|---|
| | Benzene | Toluene | $C_2$-benzene | $C_3$-benzene | $C_4$-benzene | |
| 1 | 0.015 | 0.019 | 0.022 | 0.081 | 0.085 | 1.7% |
| 2 | 0.202 | 0.028 | 0.050 | 0.068 | 0.114 | 2.1% |
| 3 | 0.069 | 0.013 | 0.051 | 0.054 | 0.068 | 1.0% |
| 4 | 0.127 | 0.055 | 0.013 | 0.007 | 0.017 | 0.6% |
| 5 | 0.074 | 0.012 | 0.082 | 0.075 | 0.108 | 1.0% |
| 6 | 0.237 | 0.213 | 0.496 | 0.018 | 0.007 | 2.8% |
| 7 | 0.164 | 0.065 | 0.014 | 0.052 | 0.077 | 1.0% |
| 8 | 0.329 | 0.072 | 0.067 | 0.124 | 0.229 | 1.6% |

[a]. measured SOA were wall loss corrected at $\omega = 0$.

Atmos. Chem. Phys. Discuss., doi:10.5194/acp-2016-50, 2016
Manuscript under review for journal Atmos. Chem. Phys.
Published: 1 March 2016


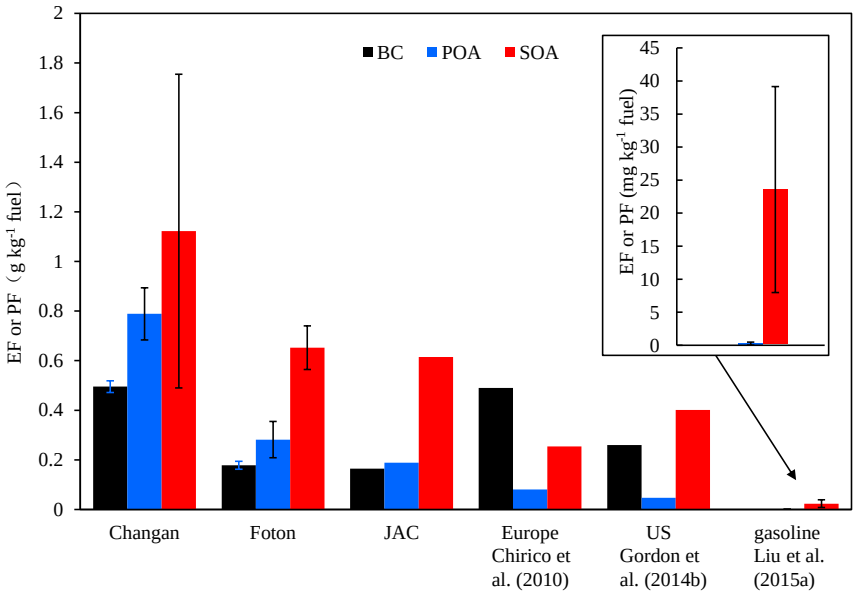


**Figure 1** Emission factors of BC and POA and production factors of SOA for ω=1from different diesel vehicle exhausts in this study, as well as those from diesel and gasoline vehicle reported in literatures. The error bars represent the ranges of EFs and PFs for each vehicle. The emission factor reported by Chirico et al. (2010) is under idling condition for a MDDV without aftertreatment. The emission factor reported by Gordon et al. (2014b) is the result under creep + idling condition for a HDDV without aftertreatment. The emission factor of gasoline is from the dataset of Liu et al. (2015a), and BC was not reported but comparatively negligible. The right-hand side of the figure shows average values from 5 gasoline vehicle experiments from Liu et al. (2015a)

Atmos. Chem. Phys. Discuss., doi:10.5194/acp-2016-50, 2016
Manuscript under review for journal Atmos. Chem. Phys.
Published: 1 March 2016


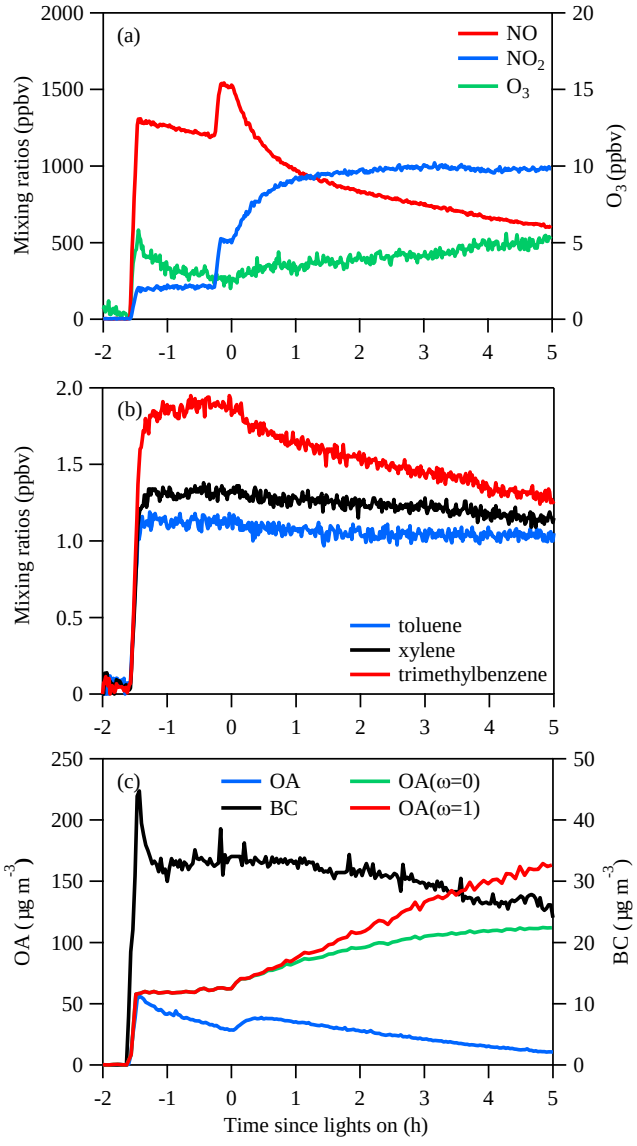


**Figure 2** Evolution of gaseous and particulate species during a typical smog chamber experiment (Experiment 8). Concentrations of (a) $NO_x$, $O_3$, (b) single-ring aromatic SOA precursors, and (c) measured OA and BC and wall loss corrected organic aerosol (OA( ω =0) and OA( ω =1)). t=0 represents the time we turned on the black lights.

Atmos. Chem. Phys. Discuss., doi:10.5194/acp-2016-50, 2016
Manuscript under review for journal Atmos. Chem. Phys.
Published: 1 March 2016


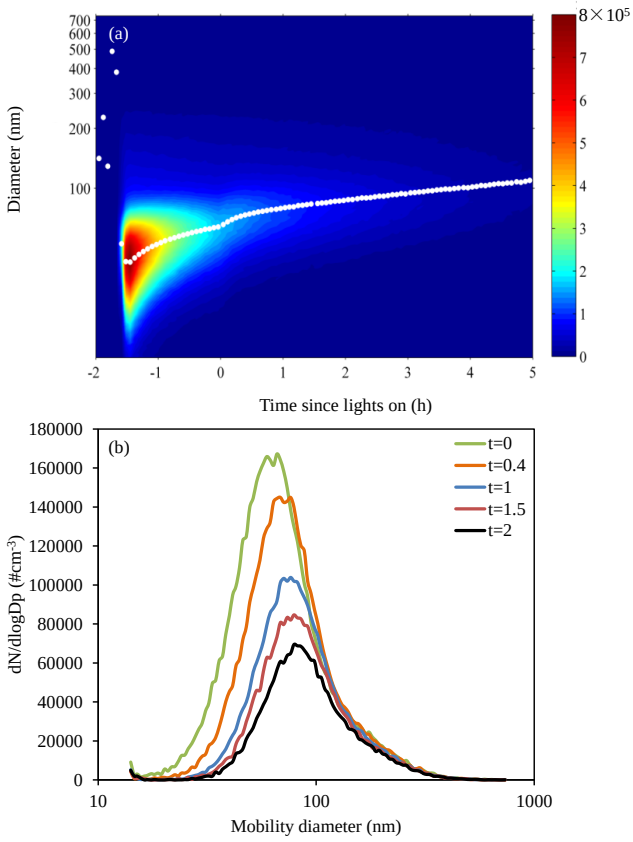


**Figure 3** (a) Particle size–number concentration distributions as a function of time. The white dots represent the evolution of median diameter during the experiment. (b) Particle number distribution in Experiment 8 at t=0 h, 0.4 h, 1 h 1.5 h and 2 h after lights were turned on.

Atmos. Chem. Phys. Discuss., doi:10.5194/acp-2016-50, 2016
Manuscript under review for journal Atmos. Chem. Phys.
Published: 1 March 2016


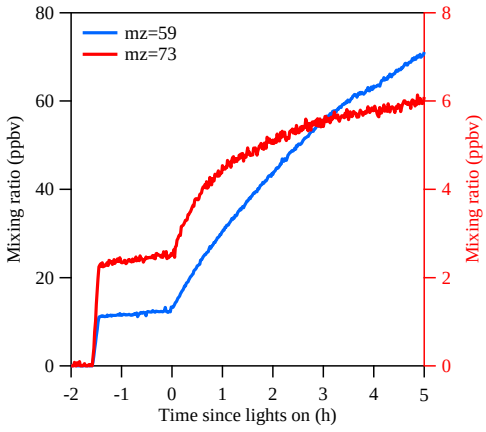


**Figure 4** The mixing ratios of ions at *m/z* 59 (acetone + glyoxal) and *m/z* 73 (methyl glyoxal) measured by PTR-MS during Experiment 8.

Atmos. Chem. Phys. Discuss., doi:10.5194/acp-2016-50, 2016
Manuscript under review for journal Atmos. Chem. Phys.
Published: 1 March 2016


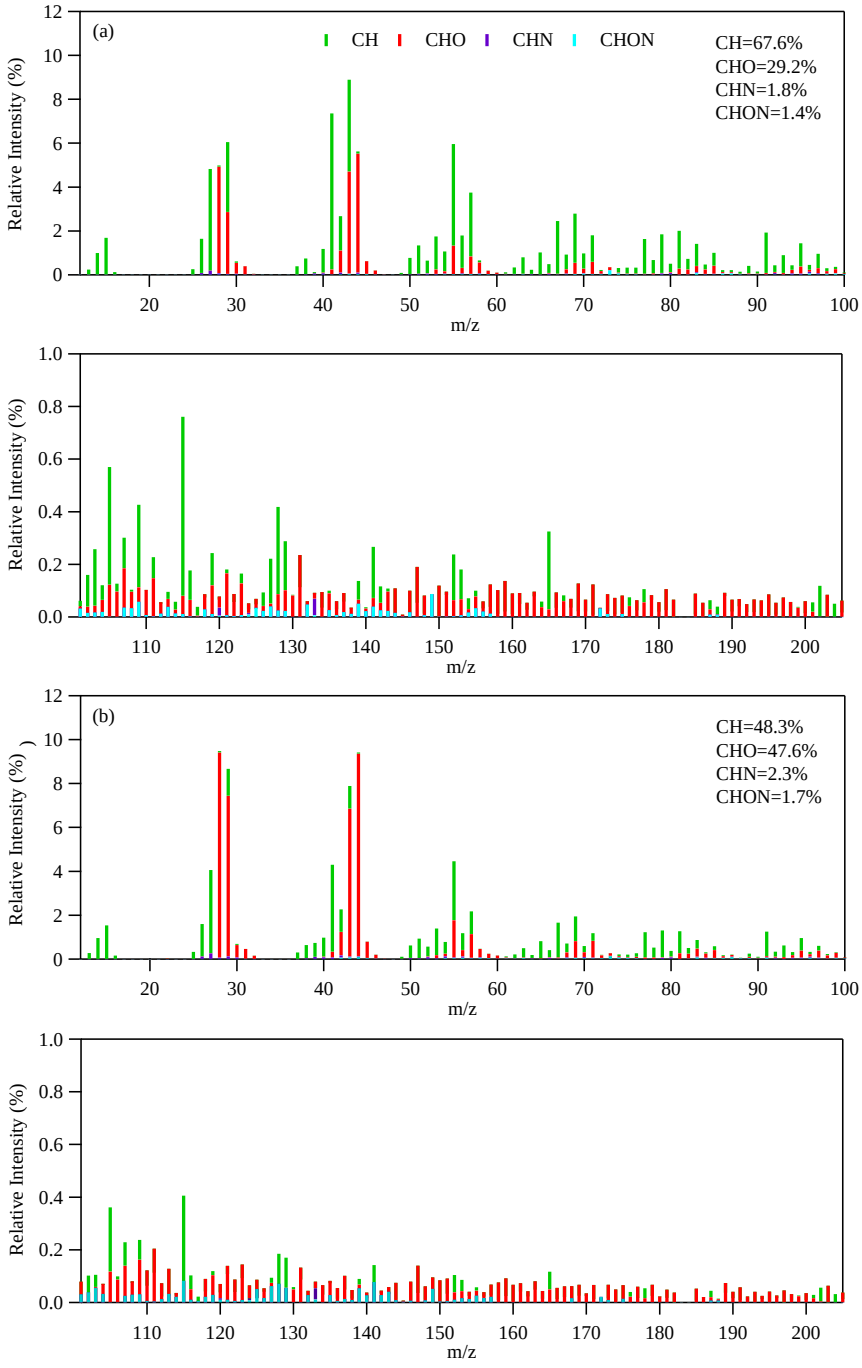


**Figure 5** Average mass spectra in high resolution (normalized to the total organic

Atmos. Chem. Phys. Discuss., doi:10.5194/acp-2016-50, 2016
Manuscript under review for journal Atmos. Chem. Phys.
Published: 1 March 2016


mass) of POA and OA after 5-hour aging measured by AMS in Experiment 8. (a) The average mass spectra of POA. (b) The average mass spectra of OA after 5 hours photo-oxidation.

Atmos. Chem. Phys. Discuss., doi:10.5194/acp-2016-50, 2016
Manuscript under review for journal Atmos. Chem. Phys.
Published: 1 March 2016


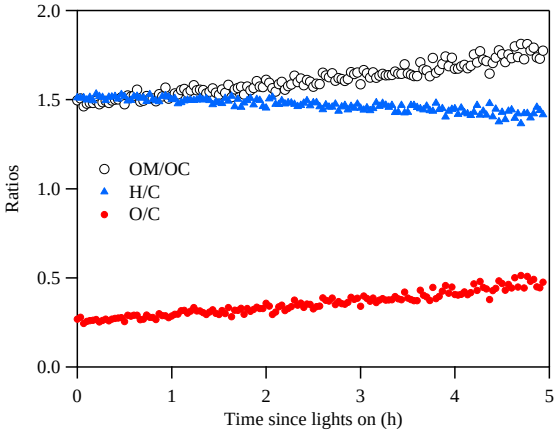


**Figure 6** Time series of average O/H and O/C atomic ratios and average OM/OC ratios during Experiment 8.

Atmos. Chem. Phys. Discuss., doi:10.5194/acp-2016-50, 2016
Manuscript under review for journal Atmos. Chem. Phys.
Published: 1 March 2016


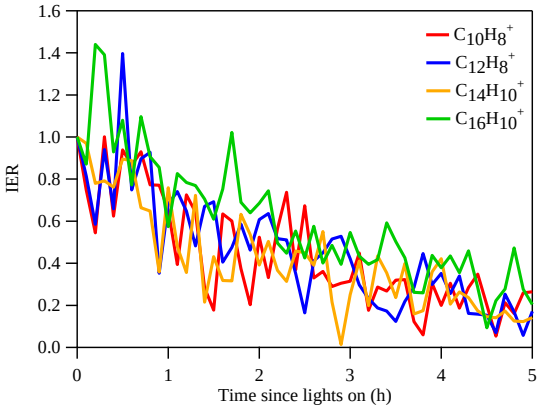


**Figure 7** Evolution of the ion enhancement ratios (IERs) of PAHs signals during Experiment 8.

Atmos. Chem. Phys. Discuss., doi:10.5194/acp-2016-50, 2016
Manuscript under review for journal Atmos. Chem. Phys.
Published: 1 March 2016


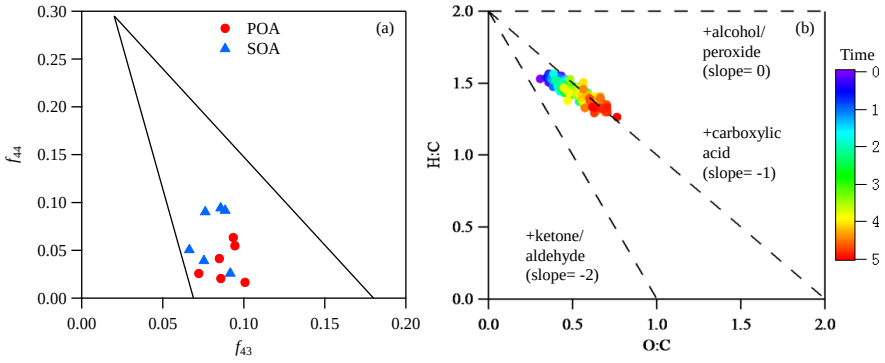


**Figure 8** (a) The fractions of total organic signal at *m/z* 43 ($f_{43}$) versus *m/z* 44 ($f_{44}$) for POA and SOA. The solid lines define the space where ambient OOA components fall. (b) The van Krevelen plot of Experiment 8. Dotted lines show slops of 0, -1 and -2. The color scale represents time evolution.